Published in final edited form as:
Cell Metab. 2011 September 7; 14(3): 313–323. doi:10.1016/j.cmet.2011.06.016.

Leptin action via neurotensin neurons controls orexin, the mesolimbic dopamine system and energy balance

Gina M. Leinninger[1,*], **Darren M. Opland**[2], **Young-Hwan Jo**[6], **Miro Faouzi**[1], **Lyndsay Christensen**[1], **Laura A. Cappellucci**[7], **Christopher J. Rhodes**[8], **Margaret E. Gnegy**[4], **Jill B. Becker**[3], **Emmanuel N. Pothos**[7], **Audrey F. Seasholtz**[3], **Robert C. Thompson**[3,5], and **Martin G. Myers Jr.**[1,2,*]

[1]Division of Metabolism, Endocrinology and Diabetes, Department of Internal Medicine, University of Michigan, Ann Arbor, MI 48109

[2]Neuroscience Program, University of Michigan, Ann Arbor, MI 48109

[3]Molecular and Behavioral Neuroscience Institute, University of Michigan, Ann Arbor, MI 48109

[4]Department of Pharmacology, University of Michigan, Ann Arbor, MI 48109

[5]Department of Psychiatry, University of Michigan, Ann Arbor, MI 48109

[6]Department of Medicine, Albert Einstein College of Medicine, Bronx, NY 10461

[7]Department of Molecular Physiology and Pharmacology, Tufts University School of Medicine, Boston, MA 02111

[8]Kovler Diabetes Center, University of Chicago, Chicago, IL 60637

Summary

Leptin acts on leptin receptor (LepRb)-expressing neurons throughout the brain, but the roles for many populations of LepRb neurons in modulating energy balance and behavior remain unclear. We found that the majority of LepRb neurons in the lateral hypothalamic area (LHA) contain neurotensin (Nts). To investigate the physiologic role for leptin action via these $LepRb^{Nts}$ neurons, we generated mice null for LepRb specifically in Nts neurons (*Nts-LepRbKO* mice). *Nts-LepRbKO* mice demonstrate early-onset obesity, modestly increased feeding, and decreased locomotor activity. Furthermore, consistent with the connection of $LepRb^{Nts}$ neurons with local OX neurons and the ventral tegmental area (VTA), *Nts-LepRbKO* mice exhibit altered regulation of OX neurons and the mesolimbic DA system. Thus, LHA $LepRb^{Nts}$ neurons mediate physiologic leptin action on OX neurons and the mesolimbic DA system, and contribute importantly to the control of energy balance.

Keywords

leptin; neurotensin; obesity; orexin; dopamine; amphetamine

*Correspondence: Martin G. Myers, Jr., M.D., Ph.D. and Gina M. Leinninger, Ph.D. Division of Metabolism, Endocrinology and Diabetes, Department of Internal Medicine University of Michigan Medical School 6317 Brehm Tower 1000 Wall St. Ann Arbor, MI 48105 PH: 734-647-9515 Fax: 734-232-8175 mgmyers@umich.edu; ggehrke@med.umich.edu.

Introduction

The increasing incidence of overweight and obesity predisposes millions of people to cardiovascular disease, type 2 diabetes and reduced life span (Farag and Gaballa, 2011; Ogden, 2006). Understanding the physiologic systems that control energy balance will be crucial to the rational development of effective therapies for obesity and related disorders. The adipose-derived hormone, leptin, acts via the long form of the leptin receptor (LepRb) to promote energy expenditure and to suppress feeding by modulating a host of neural systems and complex behaviors (Banks et al., 2000; Myers et al., 2009; Pelleymounter et al., 1995; Vaisse et al., 1996).

Commensurate with the diverse processes controlled by leptin, specialized groups of LepRb neurons lie in a variety of brain regions involved in energy balance; each LepRb population presumably modulates specific neural, physiologic and behavioral functions. LepRb neurons in mediobasal hypothalamic centers (such as the ventromedial (VMH) and arcuate (ARC) nuclei) mediate aspects of leptin action on satiety and glucose homeostasis (Balthasar et al., 2004; Coppari et al., 2005; Dhillon et al., 2006; Hill et al., 2010). The relatively modest body weight phenotype of animals null for LepRb in these mediobasal neural populations relative to the whole-body or hypothalamic deletion of LepRb suggests that other LepRb neurons contribute to the regulation of energy balance by leptin action (Balthasar et al., 2004; Berthoud, 2007; Dhillon et al., 2006; Elmquist et al., 2005; Gao and Horvath, 2007; Morton et al., 2003; Ring and Zeltser, 2010; van de Wall et al., 2008). Indeed, several populations of LepRb neurons outside of the mediobasal hypothalamus have been suggested to contribute to energy balance (Fulton et al., 2006; Hayes et al., 2010; Hommel et al., 2006; Leinninger et al., 2009).

Many aspects of physiologic leptin action remain poorly understood. For instance, leptin modulates orexin (OX; also known as hypocretin)-containing neurons (Diano et al., 2003; Louis et al., 2010; Yamanaka et al., 2003), thatregulate locomotor activity and alertness and play a crucial role in energy balance and leptin action (Yamanaka et al., 2003; Funato et al., 2009). The mesolimbic DA system also contributes to the regulation of locomotor activity, feeding and body weight, and this system is regulated, in part, by leptin and OX neurons (Fulton, et al., 2006; Hommel et al., 2006; Leinninger et al., 2009; Farooqi et al., 2009; Fadel et al., 2002; Figlewicz et al., 2007; Fulton et al., 2000; Perry et al., 2010). The mechanisms by which leptin regulates OX and the mesolimbic DA system remain poorly understood, however. Here, we address the role for physiologic leptin action via a subpopulation of LepRb neurons that contain the neuropeptide neurotensin (Nts), by generating and studying mice null for leptin action on these neurons.

Results

A neurotensin-containing subpopulation of LHA LepRb neurons

The lack of markers specific to many populations of LepRb neurons in the brain has limited the ability to genetically analyze their functions. Nts has an anatomic distribution similar to LepRb (Jennes et al., 1982; Paxinos and Franklin, 2001, Leinninger et al., 2009) in the lateral hypothalamic area (LHA). To address whether LHA LepRb neurons express Nts, we utilized $LepRb^{EGFP}$ mice (in which enhanced green fluorescent protein (EGFP) is expressed in LepRb neurons (Leinninger et al., 2009; Leshan et al., 2010; Patterson et al., 2011) to examine the potential colocalization of Nts-immunoreactivity (−IR) with LepRb, detected as GFP-IR (Figure 1A–B). This analysis revealed that many LHA LepRb neurons contain Nts-IR ($LepRb^{Nts}$ neurons). While Nts-IR was detected in many brain regions, Nts-IR only co-localized with LepRb neurons in the LHA (Supplemental Figure 1 and data not shown).

To permit the study of leptin action via $LepRb^{Nts}$ neurons, we inserted an internal ribosome entry site (IRES) plus the coding sequences for cre recombinase into the 3'-UTR of *Nts* in mice to promote Nts neuron-restricted cre expression (Nts^{cre})(Figure 1C). We bred Nts^{cre} mice with $Lepr^{fl}$ animals (McMinn et al., 2004) to generate $Nts^{cre};Lepr^{fl/fl}$ (*Nts-LepRbKO*) animals in which LepRb signaling is ablated from LHA $LepRb^{Nts}$ neurons (Figure 1C). Some of the resulting *Nts-LepRbKO* and Nts^{cre} animals were generated on the Rosa26-EGFP reporter strain (*Nts-LepRbKO*^{EGFP} and Nts^{EGFP} mice, respectively) to selectively express EGFP in Nts neurons (Nts-EGFP neurons). The analysis of EGFP expression in these animals revealed the expected broad distribution of Nts-EGFP neurons in the brain (data not shown), including a large population in the LHA (Figure 1D–I).

We examined the leptin-stimulated induction of phosphorylated signal transducer and activator-3 (pSTAT3; which reveals neurons containing functional LepRb) in EGFP-IR neurons of Nts^{EGFP} and *Nts-LepRbKO*^{EGFP} animals. Approximately 30% of LHA Nts-EGFP neurons in Nts^{EGFP} animals contained leptin-stimulated pSTAT3-IR. Conversely, approximately 60% of LHA pSTAT3/LepRb neurons colabeled with Nts-EGFP; these represent $LepRb^{Nts}$ neurons (Figure 1D). Few Nts-EGFP neurons containing pSTAT3 were detected outside of the LHA (Figure 1F, H and Supplemental Figure 1). Thus, $LepRb^{Nts}$ neurons represent a LHA-restricted subpopulation of LepRb neurons that presumably play a unique and heretofore uncharacterized role in leptin action.

While leptin-stimulated pSTAT3 outside of the LHA was unaltered in *Nts-LepRbKO*^{EGFP} mice compared to controls (Figure 1G, I), leptin-stimulated pSTAT3 in the LHA was dramatically reduced in *Nts-LepRbKO*^{EGFP} mice, and pSTAT3-IR was absent from LHA Nts-EGFP neurons in these animals (Figure 1E). Thus, functional LepRb is specifically ablated from LHA $LepRb^{Nts}$ neurons, in *Nts-LepRbKO* mice.

Direct activation of LHA $LepRb^{Nts}$ neurons by leptin

To understand the effect of leptin on the firing of $LepRb^{Nts}$ neurons, we examined the electrophysiologic response to leptin in Nts-EGFP neurons immediately above the fornix, where $LepRb^{Nts}$ neurons are concentrated, in Nts^{EGFP} and *Nts-LepRbKO*^{EGFP} animals (Figure 2). In Nts^{EGFP} mice, leptin depolarized and increased the firing of 62% of LHA Nts-EGFP neurons (n= 8/13 neurons; V_m control −58.3±3 mV, leptin −49.2±3; p=0.0003), while ~ 20% of LHA Nts-EGFP neurons responded to leptin with a slow hyperpolarization (n = 3/13 neurons; V_m control −48.4±2 mV, leptin −64.9±2; p=0.006) (Figure 2A–C). In *Nts-LepRbKO*^{EGFP} mice, however, leptin hyperpolarized all recorded LHA Nts-EGFP neurons (n = 6/6 neurons; control −47.0±4 mV, leptin −54.4±4; p=0.007) (Figure 2D, E). These data suggest that leptin directly depolarizes $LepRb^{Nts}$ neurons, while non-LepRb-expressing LHA Nts neurons are indirectly hyperpolarized by leptin; deletion of LepRb from $LepRb^{Nts}$ neurons in *Nts-LepRbKO* mice abrogates the direct depolarizing response.

Role for leptin signaling via LHA $LepRb^{Nts}$ neurons in energy homeostasis

To interrogate the contribution of LHA $LepRb^{Nts}$ neurons to leptin action, we examined energy balance and other physiologic parameters in male *Nts-LepRbKO* mice and their littermate controls ($Lepr^{fl/fl}$). *Nts-LepRbKO* mice exhibited increased body weight compared to controls (Figure 3A); this excess weight was due to increased adiposity (Figure 3B, C), while lean mass was slightly decreased as a proportion of body mass (Figure 3D). Consistent with their increased adiposity, *Nts-LepRbKO* mice also had increased circulating leptin levels (Figure 3E).

Interestingly, while (as reported previously (Balthasar et al., 2004; Dhillon et al., 2006)) no differences were observed between $Lepr^{+/+}$ and $Lepr^{fl/fl}$ animals (data not shown), $Nts^{cre/+}$

animals weighed slightly less and exhibited decreased adiposity relative to $Nts^{+/+}$ controls- suggesting a tendency of the Nts^{cre} allele to decrease body weight and adiposity (Supplemental Table 1). Thus, the increased weight and adiposity of *Nts-LepRbKO* mice is more dramatic by this comparison, since these animals possess the weight-reducing Nts^{cre} allele. Beyond body weight and adiposity, no additional effects of the Nts^{cre} allele alone were detected in our analysis (Supplemental Table 1). Thus, leptin action via $LepRb^{Nts}$ neurons contributes to the control of energy balance in mice.

Nts-LepRbKO mice exhibited slightly increased food intake at the youngest age studied, although this small difference was not detected in older animals nor was it significant when normalized to body weight (Figure 3F and data not shown). Also, *Nts-LepRbKO* mice exhibited decreased VO_2 normalized to body weight (although not on a per-animal basis (Supplemental Figure 2)) compared to control mice, especially during the dark (active) cycle, and had reduced ambulatory activity across the light-dark cycle (Figure 4A, B). In contrast, other aspects of leptin action, including measures of reproduction, growth, body temperature, and glucose homeostasis, were unperturbed in the *Nts-LepRbKO* mice (Supplemental Table 2). Thus, leptin action via $LepRb^{Nts}$ neurons participates in the regulation of energy balance in chow-fed animals via food intake and activity/energy expenditure, but does not substantially control neuroendocrine function.

LHA Nts neurons innervate the VTA and local OX neurons

To understand how $LepRb^{Nts}$ neurons might modulate brain function, we interrogated the projections of LHA Nts neurons by stereotaxically injecting the cre-inducible Ad-iZ/EGFPf virus (Leinninger et al., 2009; Leshan et al., 2010) into the LHA of Nts^{cre} mice (Figure 5A); this virus mediates the expression of farnesylated EGFP (EGFPf) in cre-containing neurons, revealing their neural projections. We found that LHA Nts neurons project locally within the LHA and caudally to the VTA (Figure 5B–E).

Since not all LHA Nts neurons contain LepRb, we examined the potential projection of LHA $LepRb^{Nts}$ neurons to the VTA by combining retrograde tracing from intra-VTA fluorogold (FG) (Supplemental Figure 4A) with immunohistochemical detection of Nts-EGFP and leptin-induced pSTAT3-IR in the LHA of Nts^{EGFP} mice (Figure 5F–I). This analysis revealed the accumulation of VTA-derived FG in EGFP-IR (Nts only) and EGFP +pSTAT3-IR ($LepRb^{Nts}$) neurons in the LHA. Thus, LHA Nts and $LepRb^{Nts}$ neurons project to the VTA.

We also interrogated whether LHA Nts neurons might project onto neurons within the LHA by injecting Ad-iN/WED (which mediates the cre-inducible expression of the trans-synaptic tracer, WGA (Louis et al., 2010) (Figure 5A)) into the LHA of Nts^{cre} mice (Figure 5 J–L, Supplemental Figure 4B). In this case, we observed numerous WGA-containing LHA neurons. We did not observe any WGA in MCH neurons (Supplemental Figure 4 C–E), suggesting that LHA Nts neurons do not contact MCH neurons. By contrast, many of the WGA-containing LHA neurons contained OX-IR, suggesting that LHA Nts neurons lie in a neuronal pathway connected to OX neurons, and might therefore modulate the function of OX neurons.

Regulation of OX neurons in *Nts-LepRbKO* mice

Leptin regulates OX neurons in two distinct manners- increasing *Ox* mRNA expression, while inhibiting the fasting-induced activity of OX neurons (as determined by c-fos expression), suggesting that diminution of ambient leptin during fasting represents a major signal to increase OX neuron activity (Diano et al., 2003; Horvath and Gao, 2005; Yamanaka et al., 2003). Thus, if $LepRb^{Nts}$ neurons mediate important aspects of physiologic

leptin action on OX neurons, fasting should not alter the activity of OX neurons of *Nts-LepRbKO* mice, since the absence of LepRb from the Nts neurons in these mice would prevent the Nts cells from detecting decreased circulating leptin. Indeed, while a 24-hour fast robustly increased c-fos in OX neurons in control animals, fasting failed to significantly change the expression of c-fos in OX neurons from *Nts-LepRbKO* mice (Figure 6A–E and antibody controls in Supplemental Figure 5).

We also treated control and *Nts-LepRbKO* mice with vehicle or leptin for 24h and examined body weight and *Ox* mRNA expression (Figure 6F,G). While leptin reduced the weight of control animals during the 24h of treatment, the weight loss was blunted in *Nts-LepRbKO* mice (Figure 6F), consistent with the role for leptin action via $LepRb^{Nts}$ neurons in regulation of body weight. Furthermore, while leptin increased *Ox* expression in control animals, this response was absent in *Nts-LepRbKO* animals (Figure 6G). Thus, leptin action via $LepRb^{Nts}$ neurons controls *Ox* expression as well as the regulation of OX neuron activity. Overall, these data suggest a central role for $LepRb^{Nts}$ neurons in the modulation of OX neurons by leptin, as well as confirming their importance in energy balance.

Altered mesolimbic DA system function in *Nts-LepRbKO* Mice

A variety of data suggest important roles for leptin in control of the mesolimbic DA system, including in the response to amphetamine (AMPH; which promotes the release of cellular DA stores via the synaptic dopamine transporter (DAT) (Figlewicz et al., 1998; Fulton et al., 2006; Kahlig et al., 2005; Sulzer et al., 1995). To determine whether physiologic leptin action via $LepRb^{Nts}$ neurons modulates the mesolimbic DA system, we examined the locomotor response of *Nts-LepRbKO* and control mice to AMPH, as well as examining other parameters of mesolimbic DA function (Figure 7). Consistent with the decreased home cage activity of *Nts-LepRbKO* mice (Figure 4B), the initial activity of *Nts-LepRbKO* mice in the locomotor chamber was reduced over the first 60 minutes of observation, although this difference in activity was absent following a vehicle injection after 60 minutes in the chamber. AMPH (IP, 4 mg/kg) rapidly increased the locomotor activity of control mice, but this effect was blunted in *Nts-LepRbKO* mice (Figure 7A), suggesting a role for $LepRb^{Nts}$ neurons in control of the mesolimbic DA system. We measured VTA *Th* expression and NAc DA content in *Nts-LepRbKO* mice to determine whether decreased mesolimbic DA might underlie the altered locomotor response to AMPH in these animals (Figure 7B, C). We found no difference in either measure in *Nts-LepRbKO* mice compared to control animals, however. We therefore used carbon fiber amperometry to examine parameters of evoked DA release in the NAc (Figure 7D,E), revealing that the amplitude of the DA peak was decreased and the $t_{1/2}$ was increased in *Nts-LepRbKO* mice compared to controls, suggesting that DAT activity is decreased in the NAc of the *Nts-LepRbKO* mice. Since the response to AMPH depends upon the availability of DAT (Giros et al., 1996; Sulzer et al., 1995; Sulzer and Rayport, 1990), these results suggest that the reduction in AMPH-induced locomotor activity could result from diminished DAT availability in the NAc of *Nts-LepRbKO* mice, and that physiologic leptin action via $LepRb^{Nts}$ neurons modulates the mesolimbic DA system at least in part by controlling DA transport.

Discussion

Our present data identify a set of Nts-expressing LepRb neurons that lie in the LHA; these $LepRb^{Nts}$ neurons are activated by leptin and are connected with local OX neurons and the VTA. By selectively deleting LepRb from $LepRb^{Nts}$ neurons in *Nts-LepRbKO* mice we demonstrate that physiologic leptin action on these LHA neurons is important for control of OX neuronal activity, *Ox* expression, mesolimbic DA function, and energy balance. Hence, $LepRb^{Nts}$ neurons mediate multiple neurophysiologic and behavioral aspects of leptin action.

The early obesity of *Nts-LepRbKO* mice and their failure to decrease body weight in response to acute leptin treatment reveal the importance of leptin action via $LepRb^{Nts}$ neurons in the control of body weight. These animals demonstrate increased body weight by 5wk of age, the only time at which a (slight) increase in food intake was detectable. While the slight lean phenotype produced by the Nts^{cre} allele likely interferes with the detection of altered energy balance in *Nts-LepRbKO* mice relative to $Lepr^{fl/fl}$ controls, the early obese phenotype of the *Nts-LepRbKO* mice suggests that their tendency toward hyperphagia and positive energy balance may be compensated by other mechanisms later in life. In adult animals, a major contributor to the maintenance of increased body weight in *Nts-LepRbKO* mice may be their decreased energy expenditure, which likely results from decreased locomotor activity. Previous reports have also suggested that leptin-mediated changes in locomotor activity can lead to altered body composition, such as the lean phenoptype of mice with constitutively active pSTAT3 in AgRP neurons (Mesaros et al., 2008) or restoration of LepRb selectively in the ARC (Coppari et al., 2005). The finding that leptin also regulates locomotor activity via LHA LepRb neurons containing Nts suggests that leptin regulation of locomotor activity is complex, and likely involves several neural pathways.

OX neurons modulate activity, and leptin regulates OX neurons (Funato et al., 2009; Louis et al., 2010; Yamanaka et al., 2003). Indeed, negative energy balance (as with fasting) activates OX neurons, and administration of exogenous leptin abrogates this fasting-induced activation, suggesting that some LepRb neuronal population inhibits OX neurons (Diano et al., 2003; Yamanaka et al., 2003). Our present findings, that $LepRb^{Nts}$ neurons lie in a pathway connected with OX neurons and regulate *Ox* expression and the activity of OX neurons, suggests that $LepRb^{Nts}$ neurons mediate important aspects of physiologic leptin action on OX neurons. Since leptin depolarizes $LepRb^{Nts}$ neurons, which contain the inhibitory neurotransmitter GABA (Leinninger et al., 2009) and innervate OX neurons, we surmise that ambient leptin in fed, energy-replete animals supports the activity of $LepRb^{Nts}$ neurons, promoting tonic GABA release onto OX neurons. During fasting, leptin levels fall, deactivating $LepRb^{Nts}$ neurons in normal animals and thus diminishing the release of GABA, thereby permitting the activation of OX neurons by glutamatergic afferents. The administration of exogenous leptin during fasting would prevent the decrease in $LepRb^{Nts}$ neuron activity and promote continued GABA release onto OX neurons, blocking their activation. Our finding that fasting fails to activate OX neurons in *Nts-LepRbKO* mice is consistent with this model, as Nts neurons in these animals are devoid of LepRb and cannot therefore sense a drop in leptin levels during food restriction. That OX neurons are not active in the fed state in the *Nts-LepRbKO* mice suggests that some form of developmental or physiological plasticity of the afferents onto OX neurons prevents the constitutive activation of these cells.

Since OX release promotes locomotor activity, it is not immediately obvious why the absence of leptin-stimulated GABA release from $LepRb^{Nts}$ neurons onto OX neurons in *Nts-LepRbKO* mice should result in the diminished activity of these animals. Possible explanations include the inability of leptin to promote increased *Ox* expression in *Nts-LepRbKO* mice; increased *Ox* expression with leptin in normal animals presumably balances the effect of decreased OX neuron firing in the leptin-replete state, maintaining the activity of the animal. This, perhaps combined with increased overall GABA innervation to prevent increased baseline activity of OX neurons in the *Nts-LepRbKO* mice, could contribute to diminished overall activity.

Chronic disruption of OX action reduces locomotor activity, thus the loss of leptin-regulated control of OX neurons may similarly impair OX-mediated behavioral output (Anaclet et al., 2009; Yamanaka et al., 2003). Indeed, leptin acts in part via OX, and action via the OX

Receptor-2 (OX2R) is required for leptin-mediated activity and body weight regulation (Funato et al., 2009; Louis et al., 2010; Yamanaka et al., 2003). Thus, the disruption of the leptin-mediated control of OX neurons in *Nts-LepRbKO* mice may represent a major contributor to the obesity of these animals. OX neurons also regulate several other physiologic parameters, such as multisynaptic relays for regulation of the sympathetic and autonomic nervous systems (including glucose metabolism/utilization), the sleep/wake cycle as well as control of motivated behaviors and addiction (Aston-Jones et al., 2009; Scammell and Winrow, 2011; Shiuchi et al., 2009). Loss of leptin-mediated control of OX neurons could, therefore, have wide-ranging physiological consequences. It is tempting to speculate that LHA LepRb^{Nts} neurons respond to leptin and other metabolic signals to accordingly regulate OX neurons, thus coupling metabolic signals with locomotor activity, arousal and behavior.

In addition to GABA, LepRb^{Nts} neurons also contain Nts. In this study we used Nts as a marker to identify and manipulate LepRb^{Nts} neurons to study their role in leptin action, though LepRb^{Nts} neurons likely mediate some effects via Nts action on downstream targets. Indeed, blockade of Nts signaling attenuates the anorectic effect of leptin, suggesting a potential role for Nts in leptin action (Kim et al., 2008; Sahu et al., 2001). While Nts and its receptors are expressed in many CNS sites (Geisler et al., 2006), most of these are not directly modulated by leptin. Thus, LHA LepRb^{Nts} neurons represent the most likely locus for Nts function in leptin action. Interestingly, a minority of LHA Nts neurons contain LepRb. Hence, LepRb^{Nts} neurons represent a subpopulation of OX-regulating LHA Nts neurons, and other subsets of LHA Nts neurons likely respond to diverse factors to control OX neurons. Hence, other physiologic modulators of OX neuron activity, such as diurnal cues, could theoretically act via LHA Nts neuron-mediated GABA release, as well.

LepRb^{Nts} neurons also innervate the VTA and modulate the mesolimbic DA system. Indeed, the suppression of AMPH-induced locomotor activity in *Nts-LepRbKO* mice is consistent with the notion that leptin action via LepRb^{Nts} neurons could underlie the stimulatory effect of leptin on the locomotor response to AMPH. Multiple mechanisms have been proposed for modulation of the AMPH response by leptin: In *Lep$^{ob/ob}$* animals, VTA *Th* expression and NAc DA content are suppressed relative to controls and leptin reverses these phenotypes (Fulton et al., 2006; Hao et al., 2004). In contrast, acute leptin treatment of normal rats is insufficient to increase DA stores, although it increases DAT activity (Perry et al., 2010). Our findings suggest that leptin action via LepRb^{Nts} neurons serves to modulate DAT function, but not DA stores. While it is possible that the alterations in DA stores in *Lep$^{ob/ob}$* mice represent a compensatory response to chronic leptin deficiency rather than a primary effect of absent leptin action, it is also possible that the non-Nts LHA LepRb neurons, which we have not examined in this study, could contribute to the regulation of DA content (or other effects) in the mesolimbic DA system. Adding further to the complexity of this system, LHA LepRb neurons likely control the mesolimbic DA system and neurophysiology by at least two mechanisms: by direct innervation of the VTA, and by the control of OX neurons (which project to the VTA, among other places (Fadel and Deutch, 2002; Peyron et al., 1998)).

Overall, our findings demonstrate important roles for leptin action via LepRb^{Nts} neurons in the control of energy balance and neurophysiology. Many of the effects on energy balance in adult *Nts-LepRbKO* animals are likely due to changes in activity that stem from impaired control of their OX and mesolimbic DA systems. Our findings also raise numerous important questions for future study regarding the neural mechanisms by which LepRb^{Nts} neurons contribute to leptin action. These issues include potential roles for Nts release by LepRb^{Nts} neurons in leptin action, potential roles for LepRb^{Nts} and other LHA Nts neurons in the control of OX neurons by non-metabolic signals, and the contribution of direct VTA

innervation by $LepRb^{Nts}$ neurons relative to indirect (via OX neurons) pathways for the control of mesolimbic DA function by leptin and $LepRb^{Nts}$ neurons.

Experimental Procedures

Materials

Leptin was the generous gift of Amylin Pharmaceuticals, Inc. (San Diego, CA). Amphetamine was from Sigma (St. Louis, MO).

Mouse Strains

$LepRb^{EGFP}$ mice have been described previously (Leinninger et al., 2009). All mice were bred and housed in a 12h light/12h dark cycle and cared for by ULAM at the University of Michigan or similar facilities at AECOM. Animals had *ad libitum* access to food and water, except for fasted animals, which had *ad libitum* access to water, but had food removed for 26 hours prior to euthanasia. All care and procedures for mice were in accordance with the guidelines and approval of the University of Michigan or AECOM University Committee on Use and Care of Animals (UCUCA).

We inserted sequences for IRES-Cre (previously described in (Leshan et al., 2006)) between the Stop codon and polyadenylation site of the sequences encoding the 3'-end of the murine *Nts* gene; a floxed Neo cassette was inserted downstream of the transcribed *Nts* gene. The Nts^{cre} construct was then linearized and electroporated into mouse R1 ES cells (129Sv background), which were selected in G418; clones were analyzed by qPCR for loss of homozygousity using Taqman primer and probes for the putative insertion site in *Nts* (Nts Forward: 5' TGA AAA GGC AGC TGT ATG AAA ATA A, Nts Reverse: 5' TCA AGA ATT AGC TTC TCA GTA GTA GTA GGA A, Nts Probe: 6FAM-CCA GAA GGC CCT ACA TTC TCA AGA GG-Tamra); *Ngf* was utilized as a copy number control, as described (Soliman et al., 2007). Putative positives were expanded, confirmed by Southern Blot, and injected into mouse C57/Bl6 blastocysts to generate chimeras. Chimeras were bred to C57/Bl6 animals (Jackson Laboratory, Bar Harbor, ME) and germline transmission was determined initially by progeny coat color, followed by confirmation by qPCR for *Nts* copy number (as described above) and conventional PCR for neo.

Experimental mice were generated by intercrossing heterozygous Nts^{cre} mice (on a mixed 129/Bl6 background) with $Lepr^{fl/fl}$ mice on the mixed C57;FVB background (the generous gift of Streamson Chua, Albert Einstein College of Medicine (McMinn et al., 2004) to generate $Nts^{cre/+}$;$Lepr^{fl/+}$ and $Lepr^{fl/+}$ animals, which we subsequently intercrossed to produce control $Lepr^{fl/fl}$ and $Nts^{cre/+}$;$Lepr^{fl/fl}$ (*Nts-LepRbKO*) mice for study. Some of these animals were generated on the *Gt(ROSA)26-*Sor^{tm2Sho} background (Nts^{cre};*Gt(ROSA)26-*Sor^{tm2Sho} (Nts^{EGFP}) and *Nts-*$LepRbKO^{EGFP}$ reporter mice) to reveal Nts neurons by EGFP expression. All of the *Nts-LepRbKO* mice and littermate controls that were studied were of mixed 129, C57/Bl6 and FVB background.

Experimental animals were genotyped for Nts^{cre} via qPCR (Cre Forward: 5' GCC GGG TCA GAA AAA ATG GT, Cre Reverse: 5' AGG GCG CGA GTT GAT AGC T, Cre Probe: 5' 6FAM-TTG GCG CGC CAT CTG CCA C-TAMRA), using *Ngf* as a copy number control. PCR was used to genotype for $Lepr^{fl}$ (mLepR- 105, mLepR-65A for $Lepr^{fl}$ and $Lepr^{+}$, respectively), and also to verify the absence of germline *Lepr* excision (referred to as $Lepr^{\Delta}$; mLepR- 105, mLepR- 106 for $Lepr^{fl}$ and $Lepr^{\Delta}$ respectively). The primers utilized herein are longer versions of those reported in (McMinn et al., 2004): mLepR-105: 5' TGA ACA GGC TTG AGA ACA TGA ACA C, mLepR-65-A: 5' AGA ATG AAA AAG TTG TTT TGG GAC GAT, mLepR-106: 5' GGT GTC TGA TTT GAT AGA TGG TCT T). The few mice found to contain $Lepr^{\Delta}$ were excluded from the study.

Immunohistochemistry and Immunofluoresence

Where noted, $LepRb^{EGFP}$ mice were treated with ICV colchicine (10 μg) as described (Leinninger et al., 2009) 2 days prior to perfusion. Mice were anesthetized with an overdose of intraperitoneal (IP) pentobarbital and transcardially perfused with 10% neutral buffered formalin. Brains were sectioned coronally (30 μm) using a freezing microtome followed by immunohistochemical or immunofluoresent analysis as described previously (Leinninger et al., 2009; Munzberg et al., 2007). DAB used for detection of pSTAT3- (Cell Signaling, rabbit, 1:250) or c-fos- (Santa Cruz, goat, 1:1000) -IR was pseudocolored using Photoshop software to appear colored in images. All other antibodies were subsequently added and visualized via immunofluorescent secondary detection using species-specific Alexa-488 or -568 antibodies (Invitrogen, 1:200) and processed and imaged as previously described (Munzberg et al., 2007). Antibodies used were GFP (Abcam, chicken, 1:1000), Nts (ImmunoStar, rabbit, 1:1000), Orexin-A (Calbiochem, rabbit, 1:2000 or Santa Cruz, goat, 1:1000), MCH (Phoenix, rabbit 1:1000), FG (Chemicon, rabbit, 1:1000) and WGA (Vector, goat, 1:1000). Controls for specificity are shown in Supplemental Figure 5.

Tract Tracing from LHA Nts^{cre} Neurons

Generation of Ad-iZ/EGFPf and Ad-iN/WED has been described previously (Leinninger et al., 2009; Louis et al., 2010). For tracing studies, adult (>8wk old) Nts^{cre} mice were administered pre-surgical analgesia (Buprenex), anesthetized with an isofluorane vaporizer and fixed in a stereotaxic apparatus before intracranial tracer administration as described (Leinninger et al., 2009; Louis et al., 2010). Coordinates to the LHA, relative to Bregma, were A/P: −1.34, M/L: −1.13, D/V: −5.20, in accordance with (Paxinos and Franklin, 2001). A similar protocol was used to deliver 10 nL of FG to the VTA of Nts^{EGFP} mice. Coordinates to the VTA, relative to Bregma, were A/P: −3.20, M/L: −0.48, D/V: −4.60, in accordance with (Paxinos and Franklin, 2001). After 2d of recovery, mice were treated with leptin (IP, 5 mg/kg, 2h), then perfused and processed for pSTAT3 by immunohistochemistry and FG and EGFP by immunofluoresence.

Slice Preparation and Electrophysiological recordings

Transverse brain slices were prepared from 21–28 day old Nts^{EGFP} and $Nts\text{-}LepRbKO^{EGFP}$ mice. Animals were anesthetized with a mixture of ketamine and xylazine. After decapitation, the brain was transferred into a sucrose-based solution bubbled with 95%O_2-5% CO_2 and maintained at ~3°C. This solution contained (m M): sucrose 248; KCl 2; $MgCl_2$ 1; $KH2PO_4$ 1.25; NaHCO3 26; sodium pyruvate 1 and glucose 10. Transverse coronal brain slices (200mM) were prepared using a vibratome. Slices were equilibrated with an oxygenated artificial cerebrospinal fluid (aCSF) for > 1 hour at 36°C prior to transfer to the recording chamber. The slices were continuously superfused with aCSF at a rate of 1.5 ml/min containing (in mM); NaCl 113, KCl 3, NaH_2PO_4 1, $NaHCO_3$ 26, $CaCl_2$ 2.5, $MgCl_2$ 1 and glucose 5 or 2.5 in 95% O_2/ 5% CO_2 at 32°C. Osmolarity was adjusted with sucrose.

Brain slices were placed on the stage of an upright, infrared-differential interference contrast microscope (Olympus BX50WI) mounted on a Gibraltar X–Y table (Burleigh). GFP-positive neurons were visualized with a 40× water immersion objective using epifluorescence imaging and patched under infrared differential interference contrast (IR-DIC) optics. Membrane potentials were recorded at 32 °C with a Multiclamp 700B in whole cell configuration. Electrophysiological signals were low-pass filtered at 10 kHz, stored on a PC and analyzed offline with pClamp 10 software (Axon instruments). Patch electrodes were pulled from thin walled glass capillaries (WPI) using a temperature controlled vertical puller (HEKA PIP5). Pipette resistance ranged from 2.5 to 4MW. The liquid junction

potential between the electrode solution and the bath solution was compensated using the pipette offset button.

CNQX (10μM), DL-amino-phosphonovaleric acid (DL-AP-5, 50μM), picrotoxin (100mM) and strychnine (1mM) (Sigma-Aldrich) were continuously present in aCSF. The internal solution contained (mM): K-acetate; 115; KCl 10; $MgCl_2$ 2; EGTA 10; HEPES 10; Na_2ATP, 2, Na_2GTP 0.5 and phosphocreatine 5. A 1000× stock solution of leptin (Sigma-Aldrich) was dissolved to final concentration in extracellular solution just before the recording session. Once a stable baseline was established after several minutes of recordings, leptin was applied by bath perfusion for 5 min at a rate of 1.5ml/min. Effects of leptin compared to control were analyzed using paired t tests (Origin 7.0).

Metabolic Phenotyping

Male mice were weaned and singly housed at 3 wk of age. Starting at 4 wk of age, mice were analyzed weekly for body weight and chow intake until they were 12 wk old. With the exception of two control mice (which were used for breeding cages), mice were then analyzed for body fat and lean mass between 12–14 wk of age using an NMR-based analyzer (Minispec LF90II, Bruker Optics). A subset of mice (13–16 wk old) was also analyzed for oxygen consumption (VO_2) and locomotor activity using the Comprehensive Laboratory Animal Monitoring System (CLAMS, Columbus Instruments). Briefly, mice were acclimated in dummy chambers for 2 d prior to being placed into the CLAMS measuring chamber for 3 d. Data represent the average values of VO_2 and X-ambulatory activity on the third day of measurement, when mice were fully acclimated to the CLAMS chamber. After a week of recovery, mice were euthanized to collect terminal serum, which was analyzed via ELISA (Crystal Chem) for insulin and leptin.

Amphetamine-Induced Locomotor Activity

Locomotor activity was assayed using Digiscan Activity Monitor chambers with light-beam sensors lining the x-, y- and z-axis of the chamber at 2.5 cm intervals (Accuscan Instruments, Columbus OH). Chambers were housed in a dedicated behavioral testing room maintained with low lighting (150 lux) during testing. Adult male mice (12–215 wk) were singly housed for >1 week prior to testing. On the morning of testing (0700 h) each mouse was placed in the chamber and allowed to habituate for the first 60 min. Next, each mouse was given an IP injection of 0.9% saline and monitored for 30 min, followed by injection of 4 mg/kg amphetamine after which activity was monitored for 90 minutes. Quantified measurements were collected in 5 min bins using the DigiPro Software Program (Accuscan Instruments, Columbus, OH). Total distance traveled by each mouse was calculated by the software.

Leptin Regulated Body Weight, Gene Expression and DA Content

Adult (10–12 wk) male mice were weighed then singly housed and treated with PBS or leptin (IP, 5 mg/kg) every 12h for 26 h total. Mice were weighed just prior to euthanasia after which brains were microdissected to obtain the LHA, VTA and NAc, which were snap-frozen and stored at −80°C. RNA was prepared from microdissected LHA and VTA using Trizol (Invitrogen) and 1 μg samples were converted to cDNA using the Superscript First Strand Synthesis System for RT-PCR (Invitrogen). Sample cDNAs were analyzed in triplicate via quantitative RT-PCR for *Gapdh* and *Ox or Th* (Applied Biosystems) using an Applied Biosystems 7500. Relative mRNA expression values are calculated by the $2^{-\Delta\Delta Ct}$ method, with normalization of each sample ΔCt value to the average ΔCt from PBS-treated control mice.

NAc tissues were assayed using high-pressure liquid chromatography (HPLC) with electrochemical detection for DA. Dialysate samples were separated on an ESA (ESA Biosciences, Chelmsford, MA) HPLC column (HR-80×3.2, 3um particle size, 80mm length) with a mobile phase consisting of: 75 mM NaH_2PO_4, 0.2 mM EDTA, 1.0~2.0mM OSA (1-octanesul fonic acid sodium salt monohydrate, Fluka Cat#74882) and 15~18% methanol (pH 5.0~5.6). Flowrate through the column was set to 1.0mL/min. DA was quantified using a coulometric detector (Coulochem II, ESA) equipped with a high sensitivity analytical cell containing dual coulometric working electrodes (ESA model #5014B). The detector settings were as follows: detector 1 −75mV, and detector 2 +100mV. Output from detector 2 was used for DA quantification.

Slice Preparation and Carbon Fiber Amperometry

A Leica VT1000S Vibratome (Leica Microsystems, Wetzlar, Germany) was used to generate 300 mm coronal brain slices immediately following brain dissection. The slices were recovered for at least one hour in artificial cerebrospinal fluid containing 124 mM NaCl, 2.0 mM KCl, 1.25 mM KH_2PO_4, 2.0 mM $MgSO_4$, 25 mM $NaHCO_3$, 1.0 mM $CaCl_2$, 11 mM Glucose, pH=7.3 (ACSF) before being placed in the recording chamber with oxygenated ACSF perfusion at 1 mL/min. A bipolar twisted wire stimulation electrode (Plastics One, Inc, Roanoke, VA, USA) and carbon fiber recording microelectrodes (manufactured as previously described (Pothos et al., 1998)) were positioned approximately 100–200 μm apart in the medial region of the NAc. Voltage was set at +700mV (Axopatch 200B; Axon Instruments, Inc., Union City, CA, USA) and a 2 msec stimulus pulse of +500 μA was administered 5 times at 5-minute intervals in each site. Data were acquired at 50 kHz and digitally postfiltered at 1 kHz (Axograph μ v.1.1.6). Amperometric peaks were identified as events greater than 3.5μ the rms noise of the baseline. The maximum amplitude (i_{max}) of the event was the highest value within the event. The width at half-height ($t_{1/2}$) was the duration of the peak from a) the baseline intercept of the maximal incline from the baseline to the first point that exceeded the cut-off and b) the first data point following the maximal amplitude that registered a value of ≤ i_{max}.

Statistics

Students' t-test was used to compare two test groups as computed with Excel. One way ANOVA with post-testing was used for multiple comparisons using In Stat software for Macintosh. Differences were considered significant for $p<0.05$.

Supplementary Material

Refer to Web version on PubMed Central for supplementary material.

Acknowledgments

We thank Amylin Pharmaceuticals (San Diego, CA) for the generous gift of leptin, Dr. Streamson Chua for the gift of *Lepr*^{fl} mice, and members of the Myers lab for helpful discussions. Core support was provided by the Michigan Diabetes Research and Training Center. Supported by grants from the American Diabetes Association and American Heart Association (MGM), the NIH (MGM, CJR, JBB, ENP), and the Obesity Society (GML).

REFERENCES

Anaclet C, Parmentier R, Ouk K, Guidon G, Buda C, Sastre JP, Akaoka H, Sergeeva OA, Yanagisawa M, Ohtsu H, et al. Orexin/hypocretin and histamine: distinct roles in the control of wakefulness demonstrated using knock-out mouse models. J Neurosci. 2009; 29:14423–14438. [PubMed: 19923277]

Aston-Jones G, Smith RJ, Moorman DE, Richardson KA. Role of lateral hypothalamic orexin neurons in reward processing and addiction. Neuropharmacology. 2009; 56(Suppl 1):112–121. [PubMed: 18655797]

Balthasar N, Coppari R, McMinn J, Liu SM, Lee CE, Tang V, Kenny CD, McGovern RA, Chua SC Jr. Elmquist JK, et al. Leptin Receptor Signaling in POMC Neurons Is Required for Normal Body Weight Homeostasis. Neuron. 2004; 42:983–991. [PubMed: 15207242]

Banks AS, Davis SM, Bates SH, Myers MG Jr. Activation of downstream signals by the long form of the leptin receptor. J Biol Chem. 2000; 275:14563–14572. [PubMed: 10799542]

Berthoud HR. Interactions between the “cognitive” and “metabolic” brain in the control of food intake. Physiology & behavior. 2007; 91:486–498. [PubMed: 17307205]

Coppari R, Ichinose M, Lee CE, Pullen AE, Kenny CD, McGovern RA, Tang V, Liu SM, Ludwig T, Chua SC Jr. et al. The hypothalamic arcuate nucleus: a key site for mediating leptin's effects on glucose homeostasis and locomotor activity. Cell Metab. 2005; 1:63–72. [PubMed: 16054045]

Dhillon H, Zigman JM, Ye C, Lee CE, McGovern RA, Tang V, Kenny CD, Christiansen LM, White RD, Edelstein EA, et al. Leptin directly activates SF1 neurons in the VMH, and this action by leptin is required for normal body-weight homeostasis. Neuron. 2006; 49:191–203. [PubMed: 16423694]

Diano S, Horvath B, Urbanski HF, Sotonyi P, Horvath TL. Fasting activates the nonhuman primate hypocretin (orexin) system and its postsynaptic targets. Endocrinology. 2003; 144:3774–3778. [PubMed: 12933647]

Elmquist JK, Coppari R, Balthasar N, Ichinose M, Lowell BB. Identifying hypothalamic pathways controlling food intake, body weight, and glucose homeostasis. J Comp Neurol. 2005; 493:63–71. [PubMed: 16254991]

Fadel J, Deutch AY. Anatomical substrates of orexin-dopamine interactions: lateral hypothalamic projections to the ventral tegmental area. Neuroscience. 2002; 111:379–387. [PubMed: 11983323]

Farag YM, Gaballa MR. Diabesity: an overview of a rising epidemic. Nephrol Dial Transplant. 2011; 26:28–35. [PubMed: 21045078]

Figlewicz DP, Patterson TA, Johnson LB, Zavosh A, Israel PA, Szot P. Dopamine transporter mRNA is increased in the CNS of Zucker fatty (fa/fa) rats. Brain Res Bull. 1998; 46:199–202. [PubMed: 9667812]

Fulton S, Pissios P, Manchon RP, Stiles L, Frank L, Pothos EN, Maratos-Flier E, Flier JS. Leptin regulation of the mesoaccumbens dopamine pathway. Neuron. 2006; 51:811–822. [PubMed: 16982425]

Funato H, Tsai AL, Willie JT, Kisanuki Y, Williams SC, Sakurai T, Yanagisawa M. Enhanced orexin receptor-2 signaling prevents diet-induced obesity and improves leptin sensitivity. Cell Metab. 2009; 9:64–76. [PubMed: 19117547]

Gao Q, Horvath TL. Neurobiology of feeding and energy expenditure. Annu Rev Neurosci. 2007; 30:367–398. [PubMed: 17506645]

Geisler S, Berod A, Zahm DS, Rostene W. Brain neurotensin, psychostimulants, and stress--emphasis on neuroanatomical substrates. Peptides. 2006; 27:2364–2384. [PubMed: 16934369]

Giros B, Jaber M, Jones SR, Wightman RM, Caron MG. Hyperlocomotion and indifference to cocaine and amphetamine in mice lacking the dopamine transporter. Nature. 1996; 379:606–612. [PubMed: 8628395]

Hao J, Cabeza de Vaca S, Carr KD. Effects of chronic ICV leptin infusion on motor-activating effects of D-amphetamine in food-restricted and ad libitum fed rats. Physiol Behav. 2004; 83:377–381. [PubMed: 15581659]

Hayes MR, Skibicka KP, Leichner TM, Guarnieri DJ, DiLeone RJ, Bence KK, Grill HJ. Endogenous leptin signaling in the caudal nucleus tractus solitarius and area postrema is required for energy balance regulation. Cell Metab. 2010; 11:77–83. [PubMed: 20074530]

Hill JW, Elias CF, Fukuda M, Williams KW, Berglund ED, Holland WL, Cho YR, Chuang JC, Xu Y, Choi M, et al. Direct insulin and leptin action on proopiomelanocortin neurons is required for normal glucose homeostasis and fertility. Cell Metab. 2010; 11:286–297. [PubMed: 20374961]

Hommel JD, Trinko R, Sears RM, Georgescu D, Liu ZW, Gao XB, Thurmon JJ, Marinelli M, DiLeone RJ. Leptin receptor signaling in midbrain dopamine neurons regulates feeding. Neuron. 2006; 51:801–810. [PubMed: 16982424]

Horvath TL, Gao XB. Input organization and plasticity of hypocretin neurons: possible clues to obesity's association with insomnia. Cell Metab. 2005; 1:279–286. [PubMed: 16054072]

Jennes L, Stumpf WE, Kalivas PW. Neurotensin: topographical distribution in rat brain by immunohistochemistry. J Comp Neurol. 1982; 210:211–224. [PubMed: 6754769]

Kahlig KM, Binda F, Khoshbouei H, Blakely RD, McMahon DG, Javitch JA, Galli A. Amphetamine induces dopamine efflux through a dopamine transporter channel. Proc Natl Acad Sci U S A. 2005; 102:3495–3500. [PubMed: 15728379]

Kim ER, Leckstrom A, Mizuno TM. Impaired anorectic effect of leptin in neurotensin receptor 1-deficient mice. Behav Brain Res. 2008; 194:66–71. [PubMed: 18639588]

Leinninger GM, Jo YH, Leshan RL, Louis GW, Yang H, Barrera JG, Wilson H, Opland DM, Faouzi MA, Gong Y, et al. Leptin acts via leptin receptor-expressing lateral hypothalamic neurons to modulate the mesolimbic dopamine system and suppress feeding. Cell Metab. 2009; 10:89–98. [PubMed: 19656487]

Leshan RL, Bjornholm M, Munzberg H, Myers MG Jr. Leptin receptor signaling and action in the central nervous system. Obesity (Silver Spring). 2006; 14(Suppl 5):208S–212S. [PubMed: 17021368]

Leshan RL, Opland DM, Louis GW, Leinninger GM, Patterson CM, Rhodes CJ, Munzberg H, Myers MG Jr. Ventral tegmental area leptin receptor neurons specifically project to and regulate cocaine- and amphetamine-regulated transcript neurons of the extended central amygdala. J Neurosci. 2010; 30:5713–5723. [PubMed: 20410123]

Louis GW, Leinninger GM, Rhodes CJ, Myers MG Jr. Direct innervation and modulation of orexin neurons by lateral hypothalamic LepRb neurons. J Neurosci. 2010; 30:11278–11287. [PubMed: 20739548]

McMinn JE, Liu SM, Dragatsis I, Dietrich P, Ludwig T, Eiden S, Chua SC Jr. An allelic series for the leptin receptor gene generated by CRE and FLP recombinase. Mamm Genome. 2004; 15:677–685. [PubMed: 15389315]

Mesaros A, Koralov SB, Rother E, Wunderlich FT, Ernst MB, Barsh GS, Rajewsky K, Bruning JC. Activation of Stat3 signaling in AgRP neurons promotes locomotor activity. Cell Metab. 2008; 7:236–248. [PubMed: 18316029]

Morton GJ, Niswender KD, Rhodes CJ, Myers MG Jr. Blevins JE, Baskin DG, Schwartz MW. Arcuate nucleus-specific leptin receptor gene therapy attenuates the obesity phenotype of Koletsky (fa(k)/fa(k)) rats. Endocrinology. 2003; 144:2016–2024. [PubMed: 12697710]

Munzberg H, Jobst EE, Bates SH, Jones J, Villanueva E, Leshan R, Bjornholm M, Elmquist J, Sleeman M, Cowley MA, et al. Appropriate inhibition of orexigenic hypothalamic arcuate nucleus neurons independently of leptin receptor/STAT3 signaling. J Neurosci. 2007; 27:69–74. [PubMed: 17202473]

Myers MG Jr. Munzberg H, Leinninger GM, Leshan RL. The geometry of leptin action in the brain: more complicated than a simple ARC. Cell Metab. 2009; 9:117–123. [PubMed: 19187770]

Ogden CL, Carroll MD, Curtin LR, McDowell MA, Tabak CJ, Flegal KM. Prevalence of overweight and obesity in the United States, 1999–2004. JAMA. 2006; 295:1549–1555. [PubMed: 16595758]

Patterson CM, Leshan RL, Jones JC, Myers MG Jr. Molecular mapping of mouse brain regions innervated by leptin receptor-expressing cells. Brain Res. 2011; 1378:18–28. [PubMed: 21237139]

Paxinos, G.; Franklin, B. The Mouse Brain in Stereotaxic Coordinates. Second Edition. Academic Press; San Diego, CA: 2001.

Pelleymounter MA, Cullen MJ, Baker MB, Hecht R, Winters D, Boone T, Collins F. Effects of the obese gene product on body weight regulation in ob/ob mice. Science. 1995; 269:540–543. [PubMed: 7624776]

Perry ML, Leinninger GM, Chen R, Luderman KD, Yang H, Gnegy ME, Myers MG Jr. Kennedy RT. Leptin promotes dopamine transporter and tyrosine hydroxylase activity in the nucleus accumbens of Sprague-Dawley rats. J Neurochem. 2010; 114:666–674. [PubMed: 20412389]

Peyron C, Tighe DK, van den Pol AN, de Lecea L, Heller HC, Sutcliffe JG, Kilduff TS. Neurons containing hypocretin (orexin) project to multiple neuronal systems. J Neurosci. 1998; 18:9996–10015. [PubMed: 9822755]

Pothos EN, Davila V, Sulzer D. Presynaptic recording of quanta from midbrain dopamine neurons and modulation of the quantal size. J Neurosci. 1998; 18:4106–4118. [PubMed: 9592091]

Ring LE, Zeltser LM. Disruption of hypothalamic leptin signaling in mice leads to early-onset obesity, but physiological adaptations in mature animals stabilize adiposity levels. J Clin Invest. 2010; 120:2931–2941. [PubMed: 20592471]

Sahu A, Carraway RE, Wang YP. Evidence that neurotensin mediates the central effect of leptin on food intake in rat. Brain Res. 2001; 888:343–347. [PubMed: 11150496]

Scammell TE, Winrow CJ. Orexin receptors: pharmacology and therapeutic opportunities. Annu Rev Pharmacol Toxicol. 2011; 51:243–266. [PubMed: 21034217]

Shiuchi T, Haque MS, Okamoto S, Inoue T, Kageyama H, Lee S, Toda C, Suzuki A, Bachman ES, Kim YB, et al. Hypothalamic orexin stimulates feeding-associated glucose utilization in skeletal muscle via sympathetic nervous system. Cell Metab. 2009; 10:466–480. [PubMed: 19945404]

Soliman GA, Ishida-Takahashi R, Gong Y, Jones JC, Leshan RL, Saunders TL, Fingar DC, Myers MG Jr. A simple qPCR-based method to detect correct insertion of homologous targeting vectors in murine ES cells. Transgenic Res. 2007; 16:665–670. [PubMed: 17570071]

Sulzer D, Chen TK, Lau YY, Kristensen H, Rayport S, Ewing A. Amphetamine redistributes dopamine from synaptic vesicles to the cytosol and promotes reverse transport. J Neurosci. 1995; 15:4102–4108. [PubMed: 7751968]

Sulzer D, Rayport S. Amphetamine and other psychostimulants reduce pH gradients in midbrain dopaminergic neurons and chromaffin granules: a mechanism of action. Neuron. 1990; 5:797–808. [PubMed: 2268433]

Vaisse C, Halaas JL, Horvath CM, Darnell JE Jr. Stoffel M, Friedman JM. Leptin activation of Stat3 in the hypothalamus of wild-type and ob/ob mice but not db/db mice. Nat Genet. 1996; 14:95–97. [PubMed: 8782827]

van de Wall E, Leshan R, Xu AW, Balthasar N, Coppari R, Liu SM, Jo YH, MacKenzie RG, Allison DB, Dun NJ, et al. Collective and individual functions of leptin receptor modulated neurons controlling metabolism and ingestion. Endocrinology. 2008; 149:1773–1785. [PubMed: 18162515]

Yamanaka A, Beuckmann CT, Willie JT, Hara J, Tsujino N, Mieda M, Tominaga M, Yagami K, Sugiyama F, Goto K, et al. Hypothalamic orexin neurons regulate arousal according to energy balance in mice. Neuron. 2003; 38:701–713. [PubMed: 12797956]

Highlights

- Neurotensin identifies a circumscribed subpopulation of LepRb neurons ($LepRb^{Nts}$).
- Loss of leptin signaling in $LepRb^{Nts}$ neurons of *Nts-LepRbKO* mice results in obesity.
- OX neurons and the mesolimbic DA system are dysregulated in *Nts-LepRbKO* mice.
- Leptin controls OX, mesolimbic DA and energy balance via $LepRb^{Nts}$ neurons.

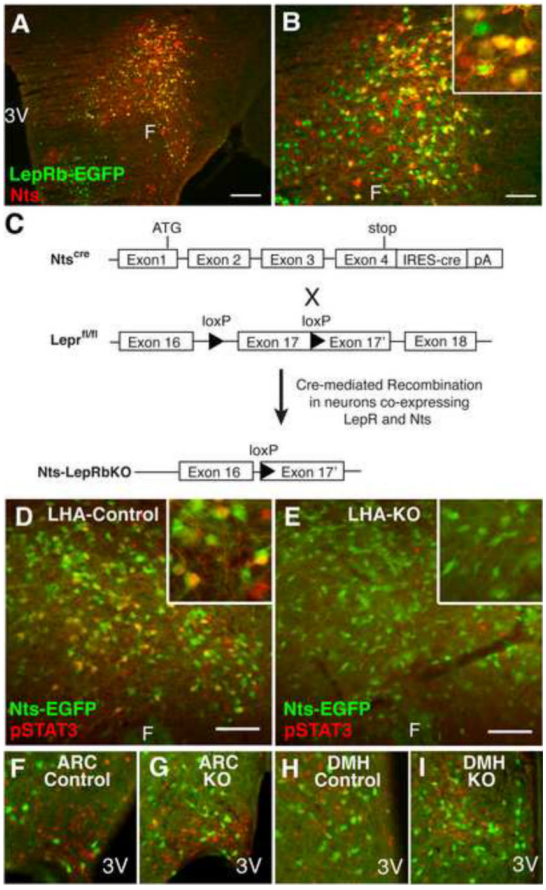

Figure 1. A Subpopulation of LHA LepRb neurons contains Nts

(A) Immunofluorescent detection of GFP (green) and Nts (red) in colchicine-treated LepRb^{EGFP} animals. (B) Enlargement of (A). (C) Schematic diagram depicting the generation of *Nts-LepRbKO* mice lacking functional LepRb only in Nts neurons. (D–I) *Nts^{cre}* mice were bred onto the Rosa26-EGFP reporter line so that cre induces the expression of EGFP to identify cre-containing (Nts) neurons. *Nts-EGFP* (Control) and *Nts-LepRbKO-EGFP* (KO) mice (n=4 each) were treated with leptin (IP, 5 mg/kg, 2h) and analyzed via immunohistochemistry for pSTAT3 (red nuclei, pseudocolored) and immunofluoresence for EGFP. (D) LHA of a leptin-treated control mouse. (E) LHA of a leptin-treated KO mouse. (F, G) Leptin-induced pSTAT3 is similar in the ARC of control (F) and KO mice (G). (H, I) Leptin-induced pSTAT3 is similar in the DMH of control (H) and KO mice (I). Insets: higher magnification view of labeled LHA neurons. Scale bar = 100 μm. 3V= third cerebral ventricle; F = fornix.

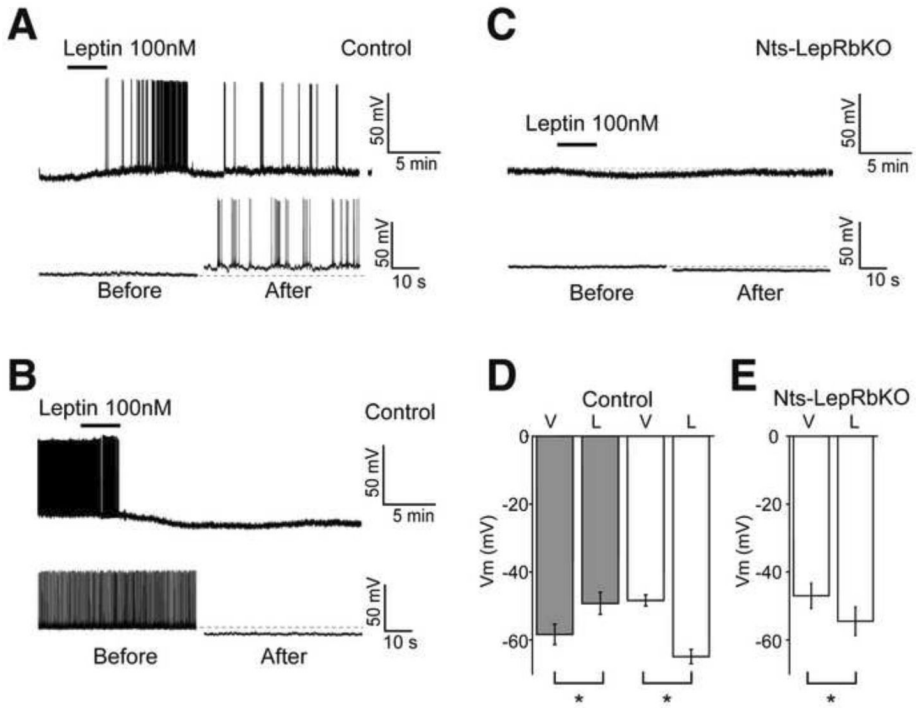

Figure 2. Electrophysiology of LHA Nts Neurons in Response to Leptin

Brain slice recordings of EGFP (i.e., Nts) neurons in the LHA of *Nts-EGFP* (Control) and *Nts-LepRbKO-EGFP* (*Nts-LepRbKO*) mice treated with vehicle (V) or leptin (100 nM, L). Representative traces (A, B, C; bottom panel, on the expanded time scale) and aggregate responses (D, E) from leptin-depolarized (A, D-grey bars) and leptin-hyperpolarized neurons (B, D- white bars) in Control mice, and (C, E) all recorded neurons in Nts-LepRbKO mice. All the recordings were performed in the presence of $GABA_A$, glycine and glutamate receptor antagonists. Data represent mean ± SEM, * = $p<0.01$ by paired t test.

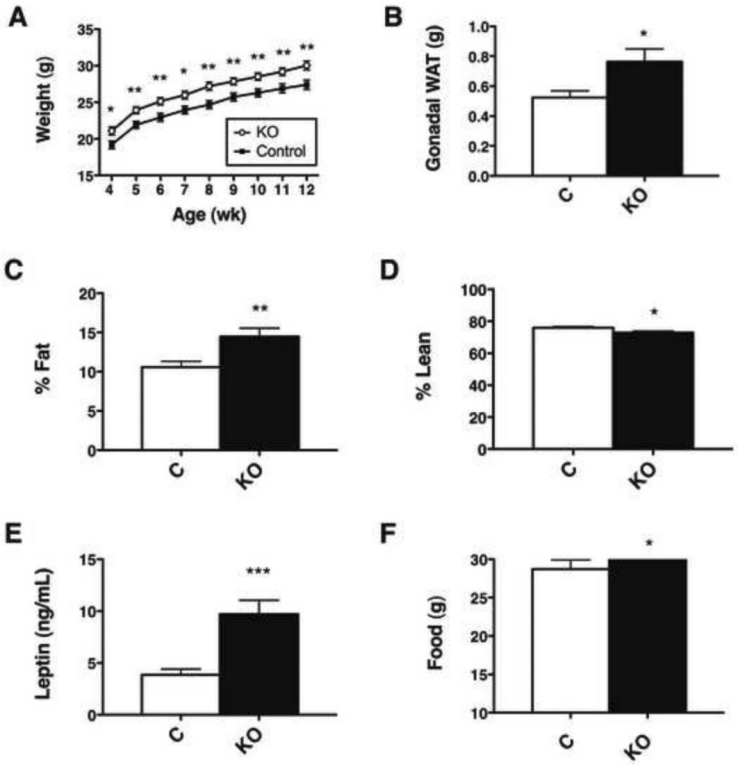

Figure 3. Leptin action via LHA LepRb^{Nts} neurons regulates body weight and adiposity via

(A) Body weight, (B) gonadal fat pad weight, (C) percentage fat mass, and (D) percentage lean mass of male Control and *Nts-LepRbKO* (KO) mice (12–14 wk old, n=23–25 per genotype). (E) ELISA analysis of terminal serum for leptin (13–15 wk old, KO n=15, control n = 16). (F) Weekly food intake from 4–5 wk of age. (n=25 per genotype). Graphed data represent average values ± SEM. *p<0.05 by Student's t test.

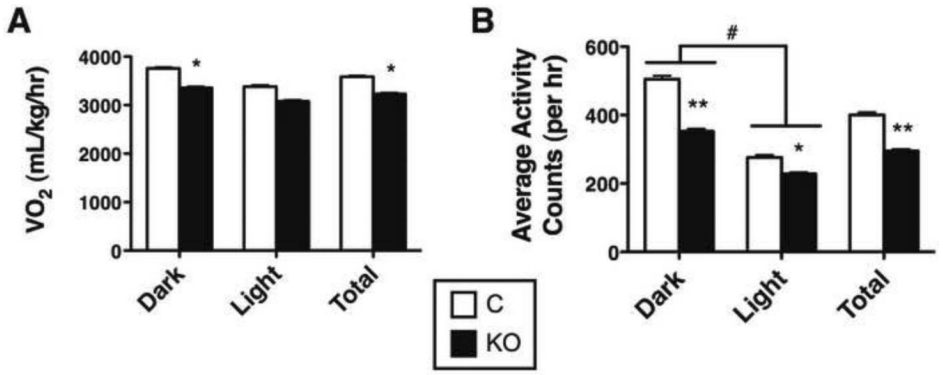

Figure 4. Leptin action via LHA LepRb^{Nts} neurons regulates VO_2 and Locomotor Activity

12–14 week old male *Nts-LepRbKO* (KO) and Control mice (KO n=20, control n = 16) were subjected to CLAMS analysis to determine (A) VO_2 and (B) ambulatory locomotor activity. Data are shown for dark cycle (Dark), light cycle (Light) and averaged over 24 hours (Total). Graphed data represent average values ± SEM. ANOVA: *p < 0.05, **p < 0.01 and ***p < 0.001 for Control vs. KO; # p<0.05 for light vs. dark.

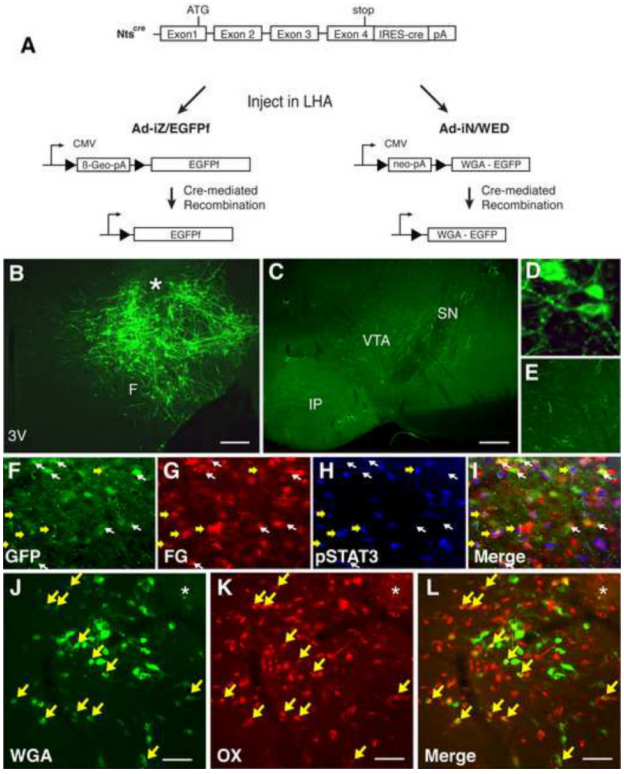

Figure 5. LHA Nts neurons project to the VTA and within the LHA onto OX neurons

(A) Schematic diagram showing cre-mediated expression of EGFPf and WGA in infected Nts-expressing neurons following stereotaxic injection of Ad-iZ/EGFPf or Ad-IN/WED, respectively, into the LHA of *Nts*^{cre} mice. (B) Immunofluorescent detection of EGFPf in the LHA of *Nts*^{cre} mice following intra-LHA injection of Ad-iZ/EGFPf identifies cell bodies and fibers (projections) in the LHA. (C) Immunofluorescent detection of EGFPf in the VTA of *Nts*^{cre} mice after intra-LHA injection of Ad-iZ/EGFPf. (D, E) Enlargements of B and D, respectively. (F–I) LHA images from leptin-treated (2h, IP, 5 mg/kg) *Nts*^{EGFP} mice injected with the retrograde tracer FG in the VTA. (F) GFP-IR, (G) FG-IR, (H) pSTAT3-IR, and (I) merged image. Yellow arrows indicate neurons positive for pSTAT3, FG and GFP. White arrows identify GFP+FG neurons that do not contain pSTAT3. (J–L) LHA from an *Nts*^{cre} mouse injected with Ad-IN/WED. (J) Immunofluoresence for WGA (green), (K) OX (red), and (L) merged. Yellow arrows: neurons that contain OX + WGA. Scale bars in (B) = 100 μm. F= fornix; 3V = third cerebral ventricle; VTA = ventral tegmental area; SN = substantia nigra (pars compacta); IP= interpeduncular tubercle; * = injection site.

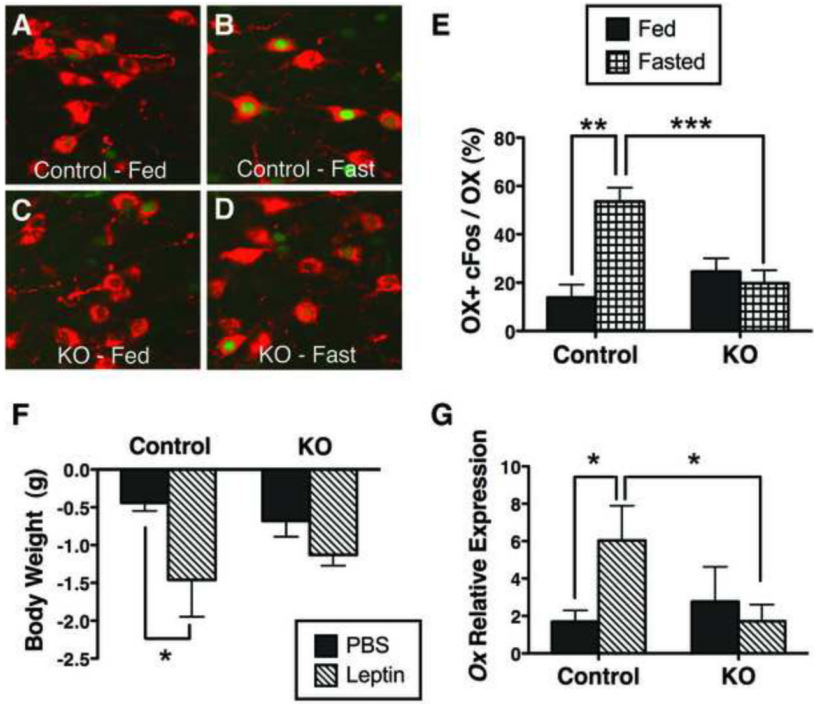

Figure 6. LHA LepRb^{Nts} neurons regulate OX neurons

Adult (12–15 wk) male *Nts-LepRbKO* (KO) and Control mice were *ad libitum* fed (A, C) or fasted for 26h (B, D) and analyzed by immunohistochemistry for cFos (green nuclei, pseudocolored) and immunofluoresence of OX neurons (red). (E) Percentage of OX neurons containing cFos in fed and fasted Control and KO mice. Control fed n= 4, control fasted n=5, KO fed n=6, KO fasted n=7. (F, G) Adult male Control and KO mice were treated with PBS or leptin (IP, 5 mg/kg) every 12h for 26 h total for the assessment of body weight and *Ox* expression. Control + PBS n=12, control + leptin n=10, KO + PBS n=12, KO + PBS n=15. (F) Weight change over 26h of treatment in control and KO mice. (G) *Ox* expression in the LHA of control and KO mice. Data are plotted as mean ± SEM; * $p<0.05$ via one-way ANOVA with Bonferroni post test.

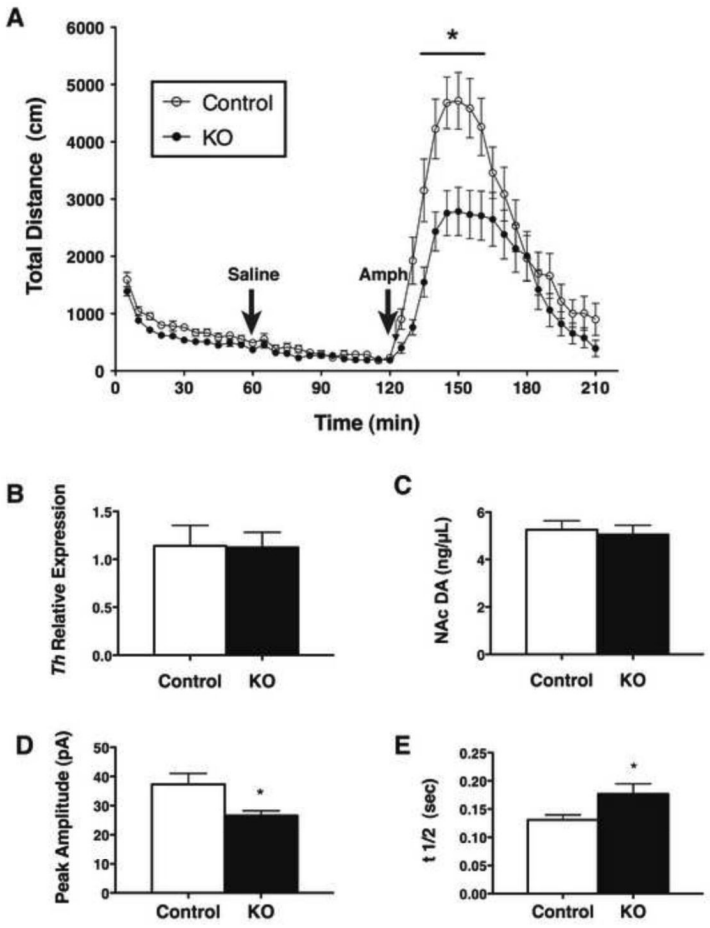

Figure 7. LHA LepRb^{Nts} neurons modulate the mesolimbic DA system

(A) Adult male *Nts-LepRbKO* (KO) and littermate Control mice were analyzed for AMPH-induced locomotor activity. Mice were placed in the activity monitoring chamber at time 0, given an IP saline injection at 60 min, AMPH (4 mg/kg, IP) at 120 minutes, and were followed for an additional 90 minutes. Graphed data represent the average total distance (cm) ambulated ± SEM, control n=15, KO n=20. (B) Relative *Th* expression in the VTA and (C) DA in the NAc of control and KO mice. Data are plotted as the average ± SEM, control n=12, Lepr^{Nts}KO n=15. (D, E) Mean evoked dopamine spike amplitude (D) and t1/2 (E) in the NAc shell in KO and Control mice. Amplitude: KO, n=36 stimulations from 8 slices in 5 animals; Control, n=42 stimulations from 9 slices in 5 animals. t1/2: KO, n=36 stimulations from 8 slices in 5 animals; Control n=42 stimulations from 9 slices in 5 animals. Data are plotted as the average ± SEM, *$p < 0.05$ by ANOVA.